Aspects of meson properties in dense nuclear matter

Octavian Teodorescu
Cornell University, Ithaca, New York 14853

Abhee K. Dutt-Mazumder
TRIUMF Theory Group, Vancouver, British Columbia, Canada

Charles Gale
McGill University, Montreal, Quebec, Canada

(Received 14 December 2001; published 26 July 2002)

We investigate the modification of meson spectral densities in dense nuclear matter at zero temperature. These effects are studied in a fully relativistic mean field model which goes beyond the linear density approximation and also includes baryon resonances. In particular, the role of $N^*(1520)$ and $N^*(1720)$ on the ρ meson spectral density is highlighted. Even though the nucleon-nucleon loop and the nucleon-resonance loop contribute with the opposite sign, an overall reduction of ρ meson mass is still observed at high density. Importantly, it is shown that the resonances cause substantial broadening of the ρ meson spectral density in matter and also induce nontrivial momentum dependence. We study the dispersion relations and collective oscillations induced by the ρ meson propagation in nuclear matter together with the influence of the mixing of ρ with the a_0 meson. The relevant expression for the plasma frequency is also recovered analytically in the appropriate limit. The spectral density of the a_0 meson is also shown.

DOI: 10.1103/PhysRevC.66.015209 PACS number(s): 25.75.Dw, 24.10.Cn, 21.65.+f

I. INTRODUCTION

Electromagnetic radiation constitutes a privileged probe of matter under extreme conditions. This owes partly to the fact that it decouples from the strongly interacting system without significant rescattering and also because the virtual photons enjoy a direct coupling to vector mesons. Lepton pairs thus carry valuable information about the in-medium properties.

Among the light vector mesons, the ρ acquires a special importance because of its large decay width. Therefore, this might serve as a chronometer and thermometer to report on transient hot and dense hadronic matter. Even though ω or ϕ mesons do not have this desired short lifetime, in the medium they might undergo sufficient broadening leading to an interesting signal [1]. For the present purpose, however, we first mostly concentrate on the ρ meson and we discuss the scalar-isovector sector later on.

The in-medium properties of the ρ meson have been estimated in a variety of models like, for example, QCD sum-rules [2], chiral models like Nambu–Jona-Lasinio, effective hadronic Lagrangian approaches [3], and mean-field models. It is fair to say that, at this point, a clear consensus is still lacking but that important progress has been realized over the past few years. For a review, see [4]. The angle of this work consists of uniting several physical aspects we find important but that had not been treated together in a unique approach. So, here, the ρ spectral density in dense nuclear matter is studied and the importance of the $N^*(1520)$ and $N^*(1720)$ is reiterated in a relativistic calculation going beyond the linear density approximation (LDA). A relativistic calculation has recently been presented in [5] in the LDA. We show that the LDA is a good approximation for densities below nuclear matter density, but for higher densities multiple scattering becomes important. We report a quantitative comparison of the results obtained in the linear approximation with a resummed one-loop calculation. We also incorporate the effect of interacting nuclear matter through the scalar and vector meson mean fields, motivated by the Walecka model. The role of resonances and that of the nucleon loops are examined separately. Finally, we include the recently discussed mixing effects [6,7], and report on the spectral density of the a_0 for the first time.

The paper is organized as follows. First the formalism is outlined followed by a discussion of the ρ meson properties involving nucleons. Then we consider the effect of the resonances on the in-medium spectral densities. Later we discuss the effect of mixing. We also present the spectral density of the a_0 meson which supplements our understanding of the mixed propagator of the ρ in nuclear matter. The calculations are done in a fully relativistic formalism including the effect of the mean field. At places the mathematical details are relegated to the Appendix. Finally we discuss the results and conclude.

II. FORMALISM

It is well known that the spectral density is actually the imaginary part of the propagator which in turn is related to the polarization functions. Therefore, we first discuss the properties of the ρ meson polarization function in dense nuclear matter.

Essentially, the spectral density is related with the collective excitation induced by the ρ meson by its propagation in nuclear matter. This is analogous to the photon propagation in a QED plasma where the propagating particle picks up the collective modes from the system arising out of the density fluctuations. This is commonly known as plasma oscillation.

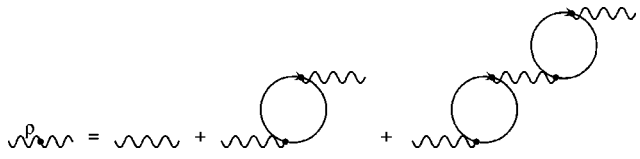

FIG. 1. Ring diagrams relevant for the random phase approximation.

Even though in the present work the main focus is not to recover the characteristic features of the plasma oscillation induced by the ρ meson, nevertheless, we outline a formalism in the manner of Chin [8] in order to be able to discuss the spectral density in terms of the dielectric response function of the nuclear matter. This enables us to incorporate the effect of meson mixing in a straightforward manner [9].

The ρ meson, being a massive spin one particle, can have both longitudinal and transverse excitations depending upon whether its momenta is perpendicular or parallel to the spin. Furthermore, in matter (unlike vacuum) these two modes will have different characteristic features. These states are designated as $\Pi^L(q_0,|\mathbf{q}|)$, $\Pi^T(q_0,|\mathbf{q}|)$ with L and T denoting longitudinal and transverse modes.

As already mentioned, we consider the coupling of ρ meson with n-n, n-R and π-π states and therefore what we have is the following:

$$\Pi^{L(T)}=\Pi^{L(T)}_{nn}+\Pi^{L(T)}_{Rn}+\Pi^{L(T)}_{\pi\pi}, \tag{1}$$

with $R=N^*(1520),N^*(1720)$, and $n=$nucleon. First we present a general formalism without the effect of mixing and later we shall address the issue of the possible mixing and of the corresponding modifications.

To describe the nuclear matter ground state we invoke the mean field approach of quantum hadrodynamics and consequently the effective nucleon mass is generated through the σ meson tadpole of the scalar mean field potential [10]. The nucleon mass is determined by solving the following equation self-consistently:

$$m_n^*=m_n-4\left(\frac{g_\sigma}{m_\sigma}\right)^2\int_0^{k_F}\frac{d^3k}{(2\pi)^3}\frac{m_n^*}{\sqrt{k^2+m_n^{*2}}}. \tag{2}$$

To study the collective excitation of the system, the relevant quantity is the dielectric function which actually characterizes the eigenvalue condition for the collective modes. In the language of field theory this is equivalent to solving the Schwinger-Dyson equation to determine the dressed propagator. The relevance of summing over the ring diagrams for the study of vector meson propagation is discussed at length in Ref. [8].

The vector meson propagation is calculated by summing over ring diagrams, a diagrammatic equivalent of the random phase approximation (RPA), which consists of repeated insertions of the lowest order polarization, as illustrated in Fig. 1 [8].

We make use of the Dyson equation to carry out the summation

$$D_{\mu\nu}(q)=D^0_{\mu\nu}(q)+D^0_{\mu\alpha}(q)\Pi^{\alpha\beta}(q)D_{\beta\nu}(q). \tag{3}$$

The poles are found from the equation

$$\det[\,\delta^\nu_\mu-D^0_{\mu\alpha}\Pi^{\alpha\nu}]=0. \tag{4}$$

The bracketed term is nothing but the dielectric tensor of the system

$$\epsilon^\nu_\mu=\delta^\nu_\mu-D^0_{\mu\alpha}\Pi^{\alpha\nu}, \tag{5}$$

the determinant of which, denoted later by $\epsilon(q)$, is the dielectric function. The eigenconditions for collective modes can now be expressed as $\epsilon(q)=0$. The relevance of the set of ring diagrams and the origin of such an eigencondition can be understood from linear response theory where the fluctuation of the current density, the source term for the meson field in nuclear matter, is ''picked up'' by the vector field.

For later convenience we define longitudinal and transverse dielectric functions as

$$\epsilon_L(q)=(1+D^0\Pi_{00})(1-D^0\Pi_{33})+D^0\Pi_{03}D^0\Pi_{30}, \tag{6}$$

$$\epsilon_T(q)=1-D^0\Pi_{11}=1-D^0\Pi_{22}=1-D^0\Pi_T. \tag{7}$$

In the above equations Π functions represent ρ meson self-energies. $D_0=1/(q^2-m_v^2)$ is the free vector meson propagator of mass m_v. The eigenmodes of the collective oscillations are given by

$$\epsilon(q)=\epsilon_T^2(q)\epsilon_L(q)=0, \tag{8}$$

corresponding to the degrees of freedom of a massive vector particle. The two identical (or degenerate) transverse collective modes are each given by

$$\epsilon_T(q)=0 \tag{9}$$

and the single longitudinal mode by

$$\epsilon_L(q)=0, \tag{10}$$

which yield the relevant dispersion curves.

A. Pion-pion loop

It is well known that the free space decay width of the ρ meson is dominantly determined by the two-pion channel. In other words its coupling to π-π loops determines the shape of the free space ρ spectral density.

The interaction between a neutral vector meson and the pions are given by (see Fig. 2)

$$\mathcal{L}=g_{\rho\pi\pi}(\pi\times\partial_\mu\pi)\cdot\rho^\mu. \tag{11}$$

The real and imaginary parts of the pion-pion loop have been discussed at length in many places; see, for example, [10] and references therein. We shall just quote the results here:

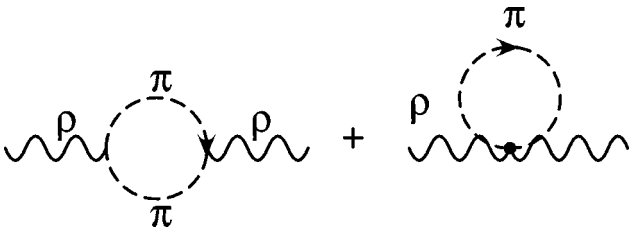

FIG. 2. ρ-$\pi\pi$ loop.

$$\mathrm{Re}\Pi^{L(T)}=\frac{g_{\rho\pi\pi}^2 M^2}{48\,\pi^2}\times\left[\left(1-\frac{4m_\pi^2}{M^2}\right)^{3/2}\ln\left|\frac{1+\sqrt{1-(1-4m_\pi^2)/M^2}}{1-\sqrt{1-(1-4m_\pi^2)/M^2}}\right|+8m_\pi^2\left(\frac{1}{M^2}-\frac{1}{m_\rho^2}\right)-2\left(\frac{q_0}{\omega_0}\right)^3\ln\left(\frac{\omega_0+p_0}{m_\pi}\right)\right], \tag{12}$$

$$\mathrm{Im}\Pi_\rho^{L(T)}=-\frac{g_{\rho\pi\pi}^2 M^2}{48\pi}\left(1-\frac{4m_\pi^2}{M^2}\right)^{3/2}. \tag{13}$$

Here $2\omega_0=m_\rho=2\sqrt{m_\pi^2+p_0^2}$.

The free-space spectral density of ρ meson is given by the following expression:

$$S_\rho(q^2)=\frac{1}{\pi}\frac{\mathrm{Im}\Sigma_\rho(q^2)}{(q^2-m_\rho^2-\Sigma_\rho)^2+\mathrm{Im}\Sigma_\rho^2}. \tag{14}$$

In vacuum, the above is a Lorentz invariant quantity and a function of q^2. In matter, however, we shall have nondegenerate spectral densities for the longitudinal and transverse mode of the ρ meson.

B. Nucleon-nucleon loop

The ρ-nucleon interaction Lagrangian may be written as (see Fig. 3)

$$\mathcal{L}_{\mathrm{int}}=g_\rho\left[\bar{N}\gamma_\mu\tau N+i\frac{\kappa_\rho}{2M}\bar{N}\sigma_{\mu\nu}\tau^\alpha N\partial^\nu\right]\rho_\alpha^\mu, \tag{15}$$

$$\Pi_{\mu\nu}^{\alpha\beta}=-ig_V^2 S_I\int\frac{d^4k}{(2\pi)^4}\mathrm{Tr}[i\Gamma_\mu^\alpha iG(k+q)i\bar{\Gamma}_\nu^\beta iG(k)], \tag{16}$$

where S_I is an isospin factor ($S_I=2$ for symmetric nuclear matter). The vertex for ρ-nn is

$$\Gamma_\mu=\gamma_\mu-\frac{\kappa_\rho}{2m_n}\sigma_{\mu\nu}q^\nu. \tag{17}$$

In Eq. (16), $G(k)$ is the in-medium nucleon propagator given by [11]

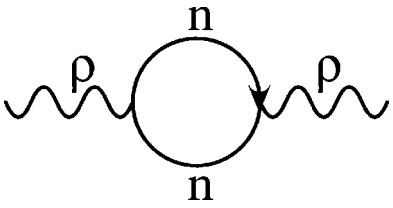

FIG. 3. ρ-nn loop.

$$G(k_0,|\vec{k}|)=G_F(k)+G_D(k_0,\vec{k}) \tag{18}$$

with

$$G_F(k)=\frac{(\not{k}+m_n^*)}{k^2-m_n^{*2}+i\epsilon} \tag{19}$$

and

$$G_D(k_0,|k|)=(\not{k}+m_n^*)\frac{i\pi}{E_k}\delta(k_0-E_k)\,\theta(k_F-|\mathbf{k}|). \tag{20}$$

The first term in $G^0(k)$, namely, $G_F^0(k)$, is the same as the free propagator of a spin $\frac{1}{2}$ particle, while the second part, $G_D^0(k)$, involving $\theta(k_F-|\vec{k}|)$, arises from Pauli blocking and describes the modifications brought about in nuclear matter at zero temperature. It deletes the on-mass-shell propagation of the nucleon in nuclear matter with momenta below the Fermi momentum [11].

When calculating the polarization function (16) with the nucleon propagator (18), there will be terms containing "G_FG_F," "$G_FG_D+G_DG_F$," and "G_DG_D." The first term accounts for the free part, i.e., the contributions of the Dirac vacuum ($\Pi_{\mu\nu}^F$), while the rest provides the density-dependent part of the polarization ($\Pi_{\mu\nu}^D$), and we can write

$$\Pi_{\mu\nu}(q)=\Pi_{\mu\nu}^F(q)+\Pi_{\mu\nu}^D(q), \tag{21}$$

$$\Pi_{\mu\nu}^F(q)=\frac{-i}{(2\pi)^4}g_V^2 S_I\int d^4k\,\mathrm{Tr}[\Gamma_\mu G_F(k+q)\bar{\Gamma}_\nu G_F(k)], \tag{22}$$

$$\Pi_{\mu\nu}^D(q)=\frac{-i}{(2\pi)^4}g_V^2 S_I\int d^4k\,\mathrm{Tr}[\Gamma_\mu G_F(k+q)\bar{\Gamma}_\nu G_D(k)+\Gamma_\mu G_D(k+q)\bar{\Gamma}_\nu G_F(k)+\Gamma_\mu G_D(k+q)\bar{\Gamma}_\nu G_D(k)]. \tag{23}$$

The free part of the ρ self-energy denoted by $\Pi_{\mu\nu}^F$ is divergent and therefore needs to be regularized. We used the dimensional regularization scheme with the following condition:

$$\partial^n\Pi^F(q^2)/\partial(q^2)^n|_{M_n^*\to M,q^2=m_s^2}=0\quad(n=0,1,2,\ldots,\infty). \tag{24}$$

The real part of the density dependent piece of the polarization is given by

$$\Pi^D_{\mu\nu}=\frac{g_v^2\pi S_I}{(2\pi)^4}\int\frac{d^4k}{E^*(k)}\delta(k^0-E^*(k))\,\theta(k_F-|\vec{k}|)\times\left[\frac{T_{\mu\nu}(k-q,k)}{(k-q)^2-M^{*2}}+\frac{T_{\mu\nu}(k,k+q)}{(k+q)^2-M^{*2}}\right]. \quad (25)$$

There is also another term which involves two $\theta(k_F-|k|)$, and which becomes operative beyond twice the Fermi energy [8].

The trace involved in the calculation of the loop diagram has three parts corresponding to vector-vector, vector-tensor and tensor-tensor terms in the vertex function (17). Those can be cast in the following forms:

$$T_{\mu\nu}=T^{vv}_{\mu\nu}(k,k+q)+T^{vt+tv}_{\mu\nu}(k,k+q)+T^{tt}_{\mu\nu}(k,k+q), \quad (26)$$

$$T^{vv}_{\mu\nu}(k,k+q)=4[k_\mu(k+q)_\nu+(k+q)_\mu k_\nu-k\cdot(k+q)g_{\mu\nu}+M^{*2}g_{\mu\nu}], \quad (27)$$

$$T^{vt+tv}_{\mu\nu}(k,k+q)=4M^*\frac{\kappa_v}{M}q^2Q_{\mu\nu}, \quad (28)$$

$$T^{tt}_{\mu\nu}(k,k+q)=16\left(\frac{\kappa_v}{4M}\right)^2[Q_{\mu\nu}(2(k\cdot q)^2-q^2k^2+q^2(k\cdot q)-q^2M^{*2})-2q^2K_{\mu\nu}], \quad (29)$$

where $\mathcal{K}_{\mu\nu}=[k_\mu-(k.q/q^2)q_\mu][k_\nu-(k.q/q^2)q_\nu)$, $Q_{\mu\nu}=(-g_{\mu\nu}+q_\mu q_\nu/q^2)$ and $E^*_k=\sqrt{\mathbf{k}^2+M^{*2}}$.

Hence the self-energy can be written as

$$\Pi^D_{\mu\nu}(q)=\Pi^{vv}_{\mu\nu}(q)+\Pi^{vt+tv}_{\mu\nu}(q)+\Pi^{tt}_{\mu\nu}(q). \quad (30)$$

The $\Pi^D_{\mu\nu}(q)$ functions in this case are as follows:

$$\Pi^{vv}_{\mu\nu}=\frac{g_v^2}{\pi^3}S_I\int_0^{k_F}\frac{d^3k}{E^*(k)}\frac{\mathcal{K}_{\mu\nu}q^2-Q_{\mu\nu}(k\cdot q)^2}{q^4-4(k\cdot q)^2}, \quad (31)$$

$$\Pi^{vt+tv}_{\mu\nu}=\frac{g_v^2}{\pi^3}S_I\left(\frac{\kappa M^*}{4M}\right)2q^4Q_{\mu\nu}\int_0^{k_F}\frac{d^3k}{E^*(k)}\frac{1}{q^4-4(k\cdot q)^2}, \quad (32)$$

$$\Pi^{tt}_{\mu\nu}=-\frac{g_v^2}{\pi^3}S_I\left(\frac{\kappa}{4M}\right)^2(4q^4)\int_0^{k_F}\frac{d^3k}{E^*(k)}\frac{\mathcal{K}_{\mu\nu}+Q_{\mu\nu}M^{*2}}{q^4-4(k\cdot q)^2}. \quad (33)$$

To include the overall degeneracy factor, the above expressions are multiplied by a factor of 2 coming from the neutron and proton loop (isospin factor). It is clear that the form for the polarization tensor conforms to the requirement of current conservation, i.e.,

$$q^\mu\Pi^D_{\mu\nu}=0=\Pi^D_{\mu\nu}q^\nu. \quad (34)$$

In the present case we observe that the free part and the dense part of the polarization tensor individually satisfy the above condition.

We should also observe that Eq. (33) is proportional to $Q_{\mu\nu}$ and therefore contributes equally to the longitudinal and transverse modes. In fact, it is $\mathcal{K}_{\mu\nu}$ which in matter induces the splitting of these two modes as we shall discuss later. Evidently, the Dirac part (vacuum) is also proportional to $Q_{\mu\nu}$ and therefore the modes remain degenerate on account of Lorentz symmetry. At $|q|=0$ they are degenerate because of rotational symmetry.

Also, it is worthwhile to point out that we could describe these effects in the linear density approximation for low baryonic densities. In this approximation, Eqs. (32)–(34) have a closed form:

$$\Pi^{vv}_{T(L)}=-4g_v^2\frac{M^*\alpha_{T(L)}}{q^4-4M^{*2}q_0^2}\rho_B, \quad (35)$$

$$\Pi^{vt+tv}_{T(L)}=4g_v^2\left(\frac{\kappa M^*}{4M}\right)\frac{q^4}{M^*(q^4-4M^{*2}q_0^2)}\rho_B, \quad (36)$$

$$\Pi^{tt}_{T(L)}=-4g_v^2\left(\frac{\kappa}{2M}\right)^2\frac{M^*q^2\beta_{T(L)}}{q^4-4M^{*2}q_0^2}\rho_B. \quad (37)$$

These results could also directly be obtained by multiplying the forward scattering amplitude with the density. Note that a nonrelativistic limit for the nucleons was taken here, in order to compare with a known result a few lines below. In the above expressions $\alpha_T=q_0^2$, $\alpha_L=q^2$ and $\beta_{T(L)}=\alpha_{L(T)}$.

To provide further insight, one can make a long wavelength approximation. When $q_0<E_F$ and $|q|<k_F$, Eq. (36) reduces to $\Pi^{vv}_{T(L)}=g_v^2/M^*\rho_B$. In this limit, with $\kappa=0$, the dispersion relation of the density dependent part alone becomes

$$q_0^2=|q|^2+m_v^2+\Omega^2, \quad (38)$$

where the plasma frequency $\Omega^2=g_v^2/M^*\rho_B$. This is the nonrelativistic result presented by Chin [8] for the case of ω meson propagation in nuclear matter. Furthermore, replacing g_v by the electronic charge "e" and putting $m_v=0$, one obtains the familiar plasma frequency encountered in condensed matter physics [12].

In Fig. 4 we compare resummed one-loop results of the ρ-meson self-energy (without kinematic approximations) with the ones calculated in the linear density approximation. The ratio of the self-energies for the transverse modes are shown as a function of density.

It is apparent that the results obtained in the linear density approximation are consistent (up to a 10% level) with exact one-loop results for nuclear matter at normal density. However, Fig. 4 indicates that for higher densities one needs to go beyond the LDA which is a popular approximation. Furthermore, a strong energy dependence manifests itself at higher densities. If one went beyond the bare one-loop and took higher in order diagrams into account, the scenario might

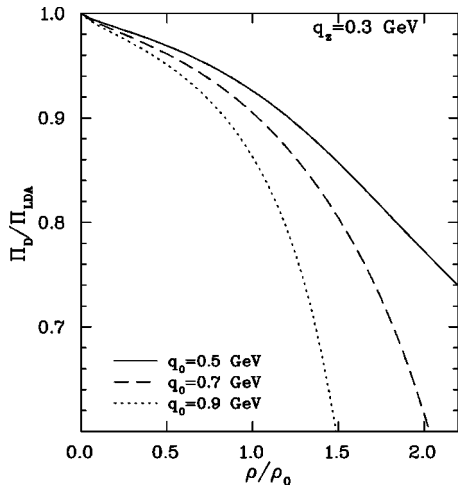

FIG. 4. Comparison of the ρ-meson self-energy calculated at the one-loop level with the one calculated in the linear density approximation.

change. It might well be the case that terms higher order in coupling might contribute differently in the density expansion. However, we leave this for future investigations.

C. Nucleon-resonance loop

In the present work, we shall consider only $N^*(1520)$ and $N^*(1720)$, as they couple strongly with the ρ meson as indicated in [13]. The corresponding relativistic interactions are given by

$$\mathcal{L}_{\rm int}=\begin{cases}\dfrac{f_{RN\rho}}{m_\rho}\bar{\psi}^\mu\gamma^\nu\psi F_{\mu\nu} & \text{for} \quad I(J^\pi)=\dfrac{1}{2}\left(\dfrac{3^-}{2}\right)\\ \dfrac{f_{RN\rho}}{m_\rho}\bar{\psi}^\mu\gamma^5\gamma^\nu\psi F_{\mu\nu} & \text{for} \quad I(J^\pi)=\dfrac{1}{2}\left(\dfrac{3^+}{2}\right).\end{cases} \tag{39}$$

Here ψ^μ denotes the resonance spinor and ψ the nucleon spinor, $\sigma^{\mu\nu}=(i/2)[\gamma^\mu,\gamma^\nu]$ and $F^{\mu\nu}=\partial^\mu\rho^\nu-\partial^\nu\rho^\mu$. $N^*(1520)$ and $N^*(1720)$ have total widths of $\sim$120 and 150 MeV, respectively, with corresponding branching ratios into the ρ-N channel of $\sim$24 and 115 MeV.

From Fig. 5 it is clear that the polarization tensor has two parts, as shown in the figure, which we refer to as the ''direct'' and ''cross'' terms. We present analytical results only for the first term, but the other term is calculated in a similar fashion:

$$-i\Pi^{\pm({\rm dir})}_{\mu\nu}=S_I\int\frac{d^4k}{(2\pi)^4}\frac{T^\pm_{\mu\nu}(k,k-q)}{(k-q)^2-m_R^2}\left[\frac{1}{k^2-m_n^2}+\frac{i\pi}{E_k}\delta(k^2-m_n^2)\theta(k_F-|k|)\right], \tag{40}$$

where S_I is the isospin factor. The vertex factors for $R^{3/2}N\rho$ can be written as

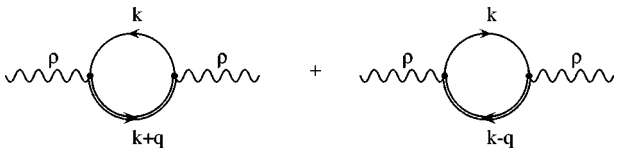

FIG. 5. ρ self-energy.

$$\Gamma^\pm_{\mu\alpha}=\frac{f_\rho}{m_\rho}(\gamma_5)^{(1\pm1)/2}(\gamma_\mu q_\alpha-\not{q}g_{\mu\alpha}). \tag{41}$$

It is clear that like the n-n loop, $\Pi^{\pm({\rm dir})}_{\mu\nu}$ also contains a ''free'' and a density-dependent part. The detailed expression for the free part is given in the Appendix and has a form $\Pi_{\mu\nu}=Q_{\mu,\nu}\Pi(q^2)$. Note also that

$$\begin{aligned}T^\pm_{\mu\nu}(k+q,k)&=Tr[i(\not{k}+m_n)i\Gamma^\pm_{\mu\alpha}i\mathcal{R}^{\alpha\beta}_{3/2}(k-q)i\Gamma^\pm_{\beta,\nu}]\\&=Tr[(\not{k}\mp m_n)(\gamma_\mu q_\alpha-\not{q}g_{\mu\alpha})(\not{k}-\not{q}+m_R)\\&\quad\times P^{\alpha\beta}_{3/2}(k-q)(q_\beta\gamma_\nu-\not{q}g_{\beta}\nu)].\end{aligned} \tag{42}$$

In the above equation $\mathcal{R}^{\mu\nu}_{3/2}(p)$ is the Rarita-Schwinger propagator, given by

$$\mathcal{R}^{\mu\nu}_{3/2}(p)=(\not{p}+m_R)P^{\mu\nu}_{3/2}(p) \tag{43}$$

$$=(\not{p}+m_R)\left[-g^{\mu\nu}+\frac{1}{3}\gamma^\mu\gamma^\nu+\frac{2}{3}\frac{p^\mu p^\nu}{m_R^2}-\frac{1}{3}\frac{p^\mu\gamma^\nu-\gamma^\mu p^\nu}{m_R}\right]. \tag{44}$$

We use the on-shell propagator, keeping in mind that there is an overall sign ambiguity with spin 3/2 particles which arises from the special choice of the point transformation properties of the spin 3/2 Lagrangian [14,15]. Appropriate discussions can also be found in Refs. [5,16,17].

The relevant trace can be written in the following suggestive form:

$$T^\pm_{\mu\nu}(k,k-q)=\left(\frac{f_\rho}{m_\rho}\right)^2\alpha^\pm Q_{\mu\nu}+\beta^\pm K_{\mu\nu}, \tag{45}$$

where

$$\begin{aligned}\alpha^\pm&=\frac{8}{3}\left[-k^2q^2+m_nm_Rq^2+\frac{k^2q^4}{m_R^2}-2\frac{k^2q^2(k\cdot q)}{m_R^2}-\frac{q^4(k\cdot q)}{m_R^2}\right.\\&\left.+(k\cdot q)^2+\frac{k^2(k\cdot q)^2}{m_R^2}+2\frac{q^2k\cdot q^2}{m_R^2}-\frac{(k\cdot q)^3}{m_R^2}\right],\\\beta^\pm&=\frac{8}{3}(k\cdot q-k^2-m_R^2)\frac{q^2}{m_R^2}.\end{aligned} \tag{46}$$

This structure is similar to what we had for the nucleon loop and therefore satisfies the condition of current conservation

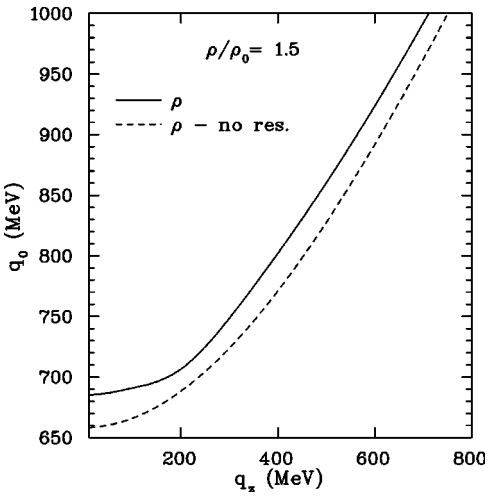

FIG. 6. The dispersion curve for ρ showing explicitly the effect of the baryonic resonances. See the text for details.

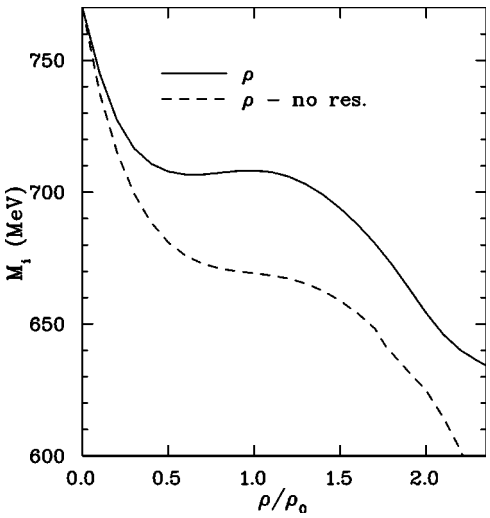

FIG. 7. The "invariant mass" of the ρ meson at $|q|=0$ as a function of density showing explicitly the effect of the baryonic resonances. The dashed line here corresponds to the case where only nucleon loop is considered. The full line represents the case when we include baryonic resonances also.

$(q^\mu \Pi_{\mu\nu}=0=\Pi_{\mu\nu}q^\nu$ in momentum space). $T^{\pm}_{\mu\nu}$ involves the same gauge invariant forms $\mathcal{K}_{\mu\nu}$ and $Q_{\mu\nu}$.

In order to evaluate $\Pi^D_{\mu\nu}$ conveniently, we choose $\vec{q}$ to be along the z axis, i.e., $q=(q_0,0,0,|\vec{q}|)$, and $k\cdot q=E^*(k)q_0-|\vec{k}||q|\chi$, where χ is the cosine of the angle between $\vec{k}$ and $\vec{q}$. After ϕ integration the nonvanishing components $\Pi^D_{\mu\nu}$ are

$$\begin{pmatrix} \Pi_{00} & 0 & 0 & \Pi_{03} \\ 0 & \Pi_{11} & 0 & 0 \\ 0 & 0 & \Pi_{22} & 0 \\ \Pi_{30} & 0 & 0 & \Pi_{33}. \end{pmatrix}. \tag{47}$$

Moreover, for isotropic nuclear matter we have $\Pi^D_{22}=\Pi^D_{33}$ and $\Pi^D_{01}=\Pi^D_{10}$, and, hence, taking all this into account, we have only two nonvanishing independent components of $\Pi^D_{\mu\nu}$, linear combinations of which gives us the longitudinal and transverse components of $\Pi^D_{\mu\nu}$: $\Pi^D_L(q)=-\Pi^D_{00}+\Pi^D_{33}$ and $\Pi^D_T(q)=\Pi^D_{11}=\Pi^D_{22}$.

We can now estimate the dispersion curves of the ρ meson in nuclear matter. As mentioned, they appear as poles in the propagator and therefore zeros of the dielectric functions shown in Eqs. (9) and (10). In Fig. 6 we show the dispersion curves for ρ meson for $\rho=1.5\rho_0$ baryonic density. It is clear that the ρ meson physical mass (when $q_z=0$) drops in nuclear matter from its free space value. The dashed curve shows the results with the n-n loop only and the solid one corresponds to the case where the direct coupling of the ρ with $N^*(1520)$ and $N^*(1720)$ is also considered. It should be noted that the resonance-particle excitations contribute with opposite signs to that of the n-n loop. This partially offsets the lowering of the ρ meson mass in nuclear matter.

Figure 7 shows the variation of the "invariant mass"[1] of the ρ meson mass as a function of nuclear density. The Dirac vacuum and the density-dependent part of the self-energy contribute with opposite signs to that of the invariant mass.

At lower densities $\Pi^F_{\mu\nu}$ is mainly responsible for the lowering of the ρ mass while at higher densities the mass again tends to increase because of $\Pi^D_{\mu\nu}$. Note that those two self-energies contribute with opposite signs. This behavior was also observed in the case of the ω and σ mesons in Ref. [9].

D. ρ-a_0 mixing via n-n loop

Before we start the discussion on the ρ-a_0 mixing involving n-n polarization in nuclear matter, we should say a few words on the a_0 coupling to the nucleon. A more detailed study of the a_0 propagation in a dense medium can be found in [6]. The interaction is described by the following Lagrangian:

$$\mathcal{L}_{\rm int}=g_{a_0}\bar{\psi}\phi_{a_0,a}\tau^a\psi, \tag{48}$$

where ψ and ϕ_{a_0} correspond to the nucleon and a_0 fields, and τ_a is a Pauli matrix. The values used for the coupling parameters are obtained from Ref. [18]. We do not invoke the coupling of a_0 to the baryonic resonances since currently this is not precisely known.

The polarization vector through which the a_0 couples to ρ via the n-n loop is obtained by evaluating the Feynman diagram in Fig. 8 and is given by

$$\Pi_\mu(q_0,|\vec{q}|)=2ig_{a_0}g_\rho\int\frac{d^4k}{(2\pi)^4}\mathrm{Tr}[G(k)\Gamma_\mu G(k+q)], \tag{49}$$

where 2 is an isospin factor. With the evaluation of the trace and after a little algebra Eq. (50) can be put into a suggestive form:

[1]Here by "invariant mass" we mean $\sqrt{q_0^2-|q|^2}$. Of course, when the meson is at rest, this defines the energy of the ρ in nuclear matter.

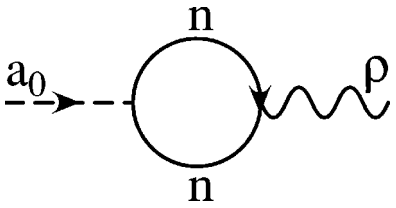

FIG. 8. a_0-ρ mixing via nucleon-nucleon loop.

$$\Pi_\mu(q_0,|q|)=\frac{g_\rho g_{a_0}}{\pi^3}2q^2\left(2m_n^*-\frac{\kappa q^2}{2m_n}\right)$$

$$\times\int_0^{k_F}\frac{d^3k}{E^*(k)}\,\frac{k_\mu-\dfrac{q_\mu}{q^2}(k\cdot q)}{q^4-4(k\cdot q)^2}. \qquad (50)$$

This immediately leads to two conclusions. First, it respects the current conservation condition, $q^\mu\Pi_\mu=0=\Pi_\nu q^\nu$. Second, there are only two components which survive the integration over azimuthal angle. This guarantees that it is only the longitudinal component of the ρ meson which couples to the scalar meson while the transverse mode remains unaltered. Furthermore, current conservation implies that out of the two nonzero components of Π_μ, only one is independent.

In the presence of mixing the combined meson propagator can be written in a matrix form where the dressed propagator would no longer be a diagonal matrix:

$$\mathcal{D}=\mathcal{D}^0+\mathcal{D}^0\Pi\mathcal{D}. \qquad (51)$$

It is to be noted that the free propagator is diagonal and has the following form:

$$\mathcal{D}^0=\begin{pmatrix}D^0_{\mu\nu} & 0\\ 0 & \Delta_0\end{pmatrix}. \qquad (52)$$

In Eq. (54) the noninteracting propagators for a_0 and ρ are given, respectively, by

$$\Delta_0(q)=\frac{1}{q^2-m_{a_0}^2+i\epsilon}, \qquad (53)$$

$$D^0_{\mu\nu}(q)=\frac{-g_{\mu\nu}+q_\mu q_\nu/q^2}{q^2-m_\rho^2+i\epsilon}. \qquad (54)$$

In fact, it is the polarization matrix which involves nondiagonal elements as shown below, characterizing the mixing

$$\Pi=\begin{pmatrix}\Pi^\rho_{\mu\nu}(q) & \Pi_\nu(q)\\ \Pi_\mu(q) & \Pi^{a_0}(q)\end{pmatrix}. \qquad (55)$$

After ϕ integration the nonvanishing components Π are

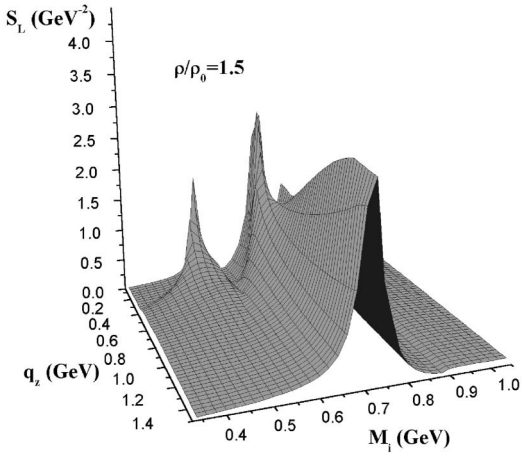

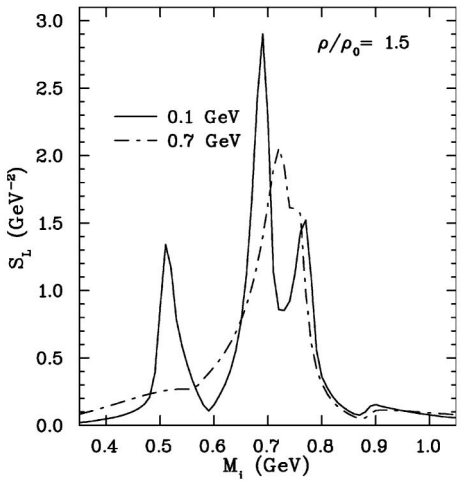

FIG. 9. The longitudinal spectral density for the ρ meson with mixing at density $\rho=1.5\rho_0$.

$$\begin{pmatrix}\Pi_{00} & 0 & 0 & \Pi_{03} & \Pi_0\\ 0 & \Pi_{11} & 0 & 0 & 0\\ 0 & 0 & \Pi_{22} & 0 & 0\\ \Pi_{30} & 0 & 0 & \Pi_{33} & \Pi_3\\ \Pi_0 & 0 & 0 & \Pi_3 & \Pi^{a_0}\end{pmatrix}. \qquad (56)$$

For the a_0 meson, the free part of the self-energy is given by

$$\Pi^{a_0}(q^2)=\frac{3g_{a_0}^2}{2\pi^2}\Bigg[3(m^{*2}-m^2)-4(m^*-m)m-(m^{*2}-m^2)$$

$$\times\int_0^1 dx\,\ln\left[\frac{m^{*2}-x(1-x)q^2}{m^2-x(1-x)q^2}\right]-\int_0^1 dx$$

$$\times(m^2-x(1-x)q^2)\ln\left[\frac{m^{*2}-x(1-x)q^2}{m^2-x(1-x)q^2}\right]. \qquad (57)$$

To determine the collective modes, one defines the dielectric function in the presence of the mixed terms [8]:

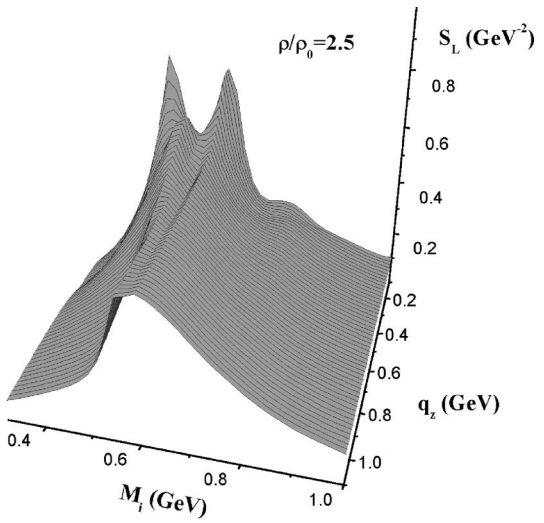

FIG. 10. The longitudinal spectral density for the ρ meson with mixing at density $\rho=2.5\rho_0$.

$$\epsilon(q_0,|\vec{q}|)=\det(1-\mathcal{D}^0\Pi)=\epsilon_T^2\times\epsilon_{\rm mix}, \tag{58}$$

where ϵ_T corresponds to two identical transverse (T) modes and $\epsilon_{\rm mix}$ correspond to the longitudinal mode with the mixing. The latter also characterizes the mode relevant for the a_0 propagation:

$$\epsilon_T=1-d_0\Pi_T, \quad d_0=\frac{1}{q^2-m_\rho^2+i\epsilon},$$

$$\epsilon_{\rm mix}=(1-d_0\Pi_L)(1-\Delta_0\Pi_s)-\frac{q^2}{|\vec{q}|^2}\Delta_0 d_0(\Pi_0)^2. \tag{59}$$

It is evident that only the longitudinal component gets modified because of the mixing, and when $\Pi_0=0$ we recover the same expression as Eq. (10).

III. ρ SPECTRAL DENSITY IN NUCLEAR MATTER

Unlike in free space, the longitudinal and transverse ρ spectral densities are nondegenerate and they are functions of q_0 and $|\mathbf{q}|$, independently. Furthermore, in matter the scalar and vector mesons can mix. This also modifies the longitudinal ρ spectral density through the off-diagonal mixing terms in Eq. (56).

Now in the presence of mixing, the spectral densities can be defined in terms of the dielectric function as

$$S_L(q_0,|\mathbf{q}|,\rho_B)=-\frac{1}{\pi}{\rm Im}\left[\frac{d_0(1-\Delta_0\Pi_s)}{\epsilon_{\rm mix}}\right]. \tag{60}$$

On the other hand, the transverse spectral density is unaffected by the mixing and has the following form:

$$S_T(q_0,|\mathbf{q}|,\rho_B)=-\frac{1}{\pi}{\rm Im}\left[\frac{d_0}{1-d_0\Pi_T}\right]. \tag{61}$$

Figure 9 shows the longitudinal spectral density (S_L) at a density $\rho=1.5\rho_0$ as a function of three momenta ($|\mathbf{q}|=q_z$) and invariant mass (M_i). This includes the effect of n-n loop and the direct coupling of the ρ meson with $N^*(1520)$ and $N^*(1720)$. The three-peak structure of the spectral density is similar to what has already been observed in nonrelativistic calculations in Refs. [19,20]. Such a characteristic behavior of the spectral density in the presence of resonance has been also observed in pion-nucleon dynamics. The collective modes induced by the density fluctuations can be identified as the ρ meson mode and N-resonance modes. Individual contributions of the resonances to the in-medium ρ spectral function are shown again in Fig. 11, but at a different density.

Figure 10 is as Fig. 9 but for higher density. We note that at higher density the spectral density gets even broader. Furthermore, with increasing momenta all the peaks merge into one broad peak, indicating the fact that at high momenta the collective behavior dies down and the meson shows a behavior of a free propagation in matter.

Next we show how individual resonant states modify the ρ spectral density in matter. In Fig. 11, the dashed-dotted line represents the ρ spectral density for ρ coupled only to the π-π and n-n loop. This shows the ρ meson peak shifts to-

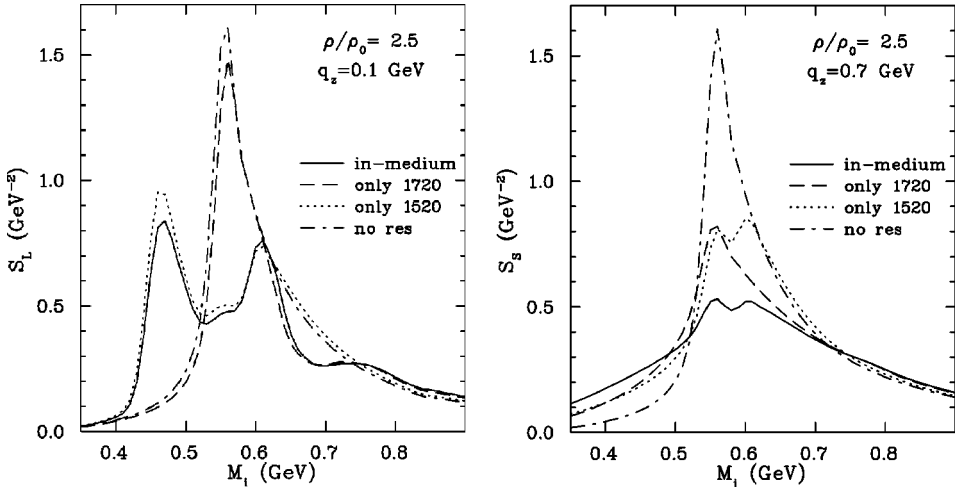

FIG. 11. The longitudinal spectral density for the ρ meson with mixing at density $\rho=2.5\rho_0$ with and without considering resonances.

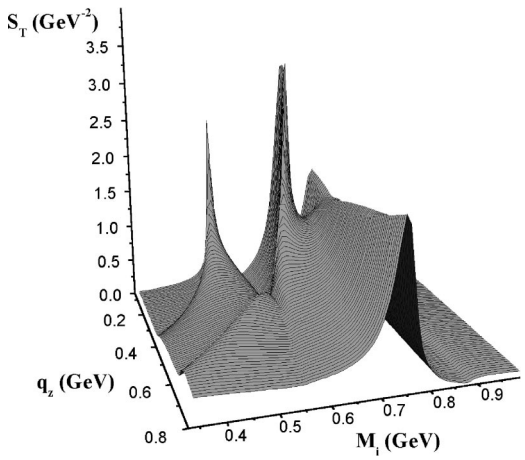

FIG. 12. The transverse spectral density for the ρ meson with mixing at density $\rho=1.5\rho_0$.

wards lower invariant mass. Similarly dotted and dashed curves correspond to the cases when we have $N^*(1520)$ and $N^*(1720)$ as indicated in the figure.

The shift owes to the σ meson mean field which lowers the nucleon mass considerably in nuclear matter. Also note that dotted curve has a double-hump structure with the introduction of the $N^*(1520)$. For nonrelativistic calculations, such a feature had been observed in [13]. The addition of the baryonic resonance also moves strength to the low invariant mass region. Hence we conclude that the resonant states are largely responsible for the broadening of the ρ spectral density in nuclear matter. Furthermore, in the presence of the resonant states the ρ meson gets broadened so much that the interpretation of the ρ meson as a good quasiparticle fails to carry any sense.

The transverse spectral density (S_T) also shows interesting features at low momenta. Again we observe that at higher momenta the ρ-spectral density gets flattened. The momentum dependence of S_T is also observed to be different than that of S_L (see Figs. 12 and 13). At higher densities we see even more pronounced effects as shown in Fig. 13.

The spectral density for the a_0 meson is defined as

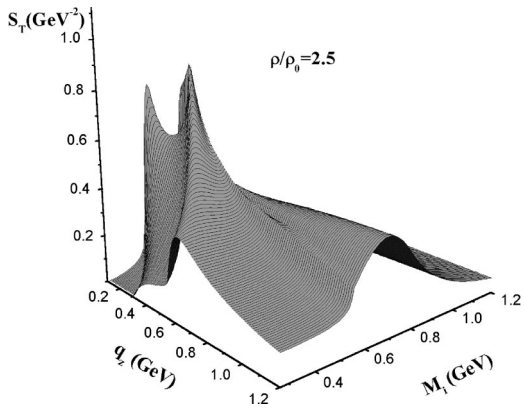

FIG. 13. The transverse spectral density for the ρ meson with mixing at density $\rho=2.5\rho_0$.

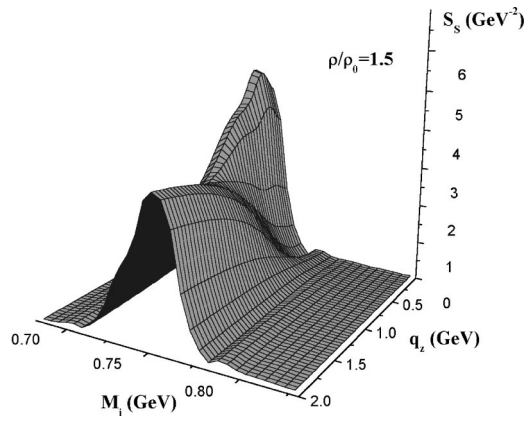

FIG. 14. Spectral density for the a_0 meson with mixing at density $\rho=1.5\rho_0$.

$$S_S(q_0,|\mathbf{q}|,\rho_B)=-\frac{1}{\pi}\mathrm{Im}\left[\frac{\Delta_0(1-d_0\Pi_S)}{\epsilon_{\mathrm{mix}}}\right]. \tag{62}$$

In Figs. 14 and 15 the spectral densities of the a_0 meson are presented at densities $\rho=1.5\rho_0$ and $\rho=2.5\rho_0$. It is evident that the a_0 spectral density also gets broadened in medium. A marked shift towards the lower invariant mass indicates that the a_0 mass also drops in nuclear matter.

To illustrate the spectral density modification in matter, we present S_L as a function of density. The solid line in Fig. 16 shows the free ρ spectral density. We find that with increasing density it acquires more strength in the low invariant mass region and also becomes flattened. Dashed, dotted, and dashed-dotted lines represent results for 0.5, 1.5, and 2.5 normal nuclear matter densities. A small peak appears in the higher invariant mass region, which indicates the effect of mixing.

In Fig. 17, the two-dimensional projection of the a_0 spectral density at $|\mathbf{q}|=0.7$ GeV ($c=1$) shows that with increasing density a_0 gets narrower and moves towards low invariant mass region. This is understandable from the reduction of

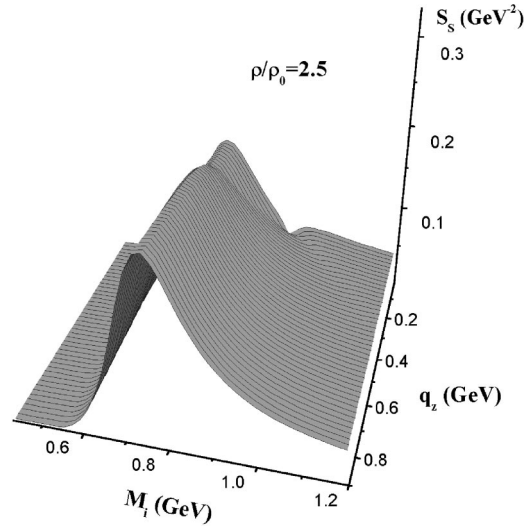

FIG. 15. Spectral density for the a_0 meson with mixing at density $\rho=2.5\rho_0$.

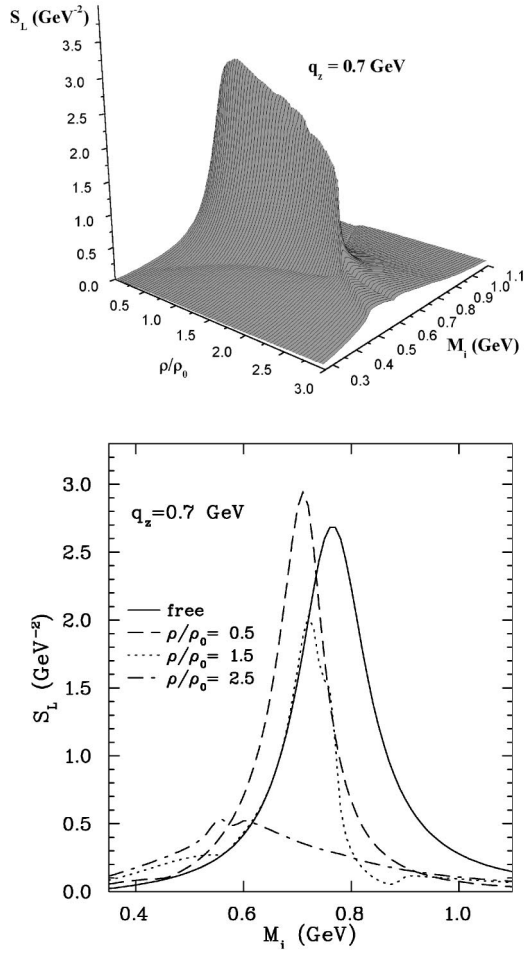

FIG. 16. The longitudinal spectral density for the ρ meson with mixing as a function of density.

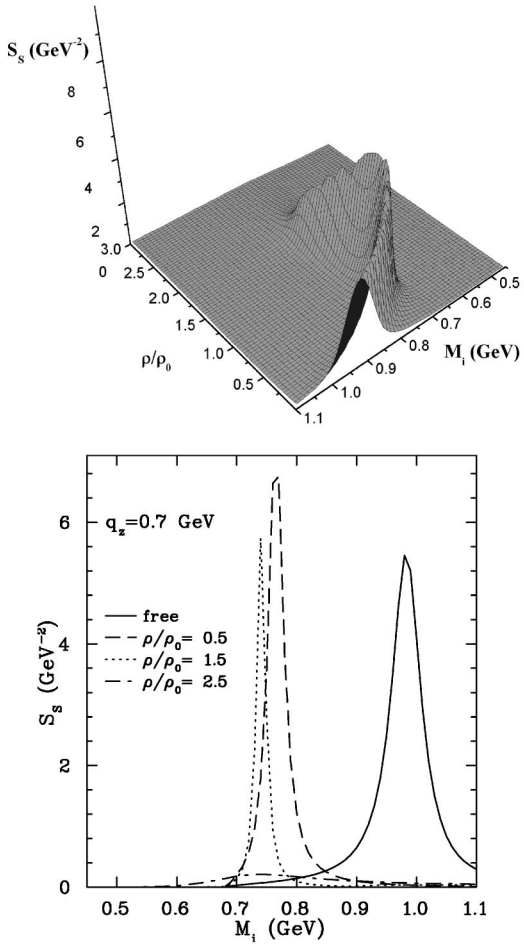

FIG. 17. The spectral density for the a_0 meson with mixing as a function of density (upper part) and a cross section for different densities (lower part).

phase space. It might be recalled here that resonant states do not couple to a_0 and therefore we do not observe any broadening in the a_0 channel.

IV. SUMMARY AND CONCLUSIONS

In the present work we present quantitative results of the in-medium meson properties. The meson spectral densities are evaluated for the first time in a fully relativistic mean field model which goes beyond linear density approximation and we discuss the limitation and applicability of the LDA. We find that meson spectral densities in matter are quite different from those in free space. The difference stems partly from the existence of a preferred frame attached to the nuclear matter. While in free space the transverse and longitudinal component of the ρ spectral density are degenerate, in matter they show different qualitative behaviors. Furthermore, we include other purely in-medium effects, forbidden in vacuum on the account of Lorentz symmetry, like meson mixing. In matter the ρ can also be modified because of its mixing with a scalar (isovector) a_0 meson. This effect, as we have seen, modifies only the longitudinal component of the spectral density.

In our model we observe that the ρ meson spectral density gets flattened in nuclear matter with the incorporation of the resonant states like $N^*(1520)$ and $N^*(1720)$. In fact, in strongly interacting matter, the original distribution of the ρ can become so broad that it is no longer possible to interpret as a quasi-particle excitation. This was also observed in Refs. [5,13]. It should also be noted that in the presence of the scalar mean field the ρ meson mass goes down as a function of density.

This broadened ρ spectral density shows an accumulation of strength towards the lower invariant mass region. This would definitely imply production of dileptons with low invariant masses in excess of what we might expect from the free ρ spectral density. We plan to extend this work to the finite temperature region in the near future. Furthermore, the broadened ρ spectral density would also affect the width of the resonance states like $N^*(1520)$ or $N^*(1720)$ which probably would shed some light on the issue of mixing resonant states in the photoabsorption cross-sections. For the complete determination of the ρ spectral density and the broadening of the resonant state, a self-consistent approach should be adopted [5]. Studies along such directions are in progress.

ACKNOWLEDGMENTS

This work was supported in part by the Natural Sciences and Engineering Research Council of Canada and in part by the Fonds FCAR of the Québec Government.

APPENDIX A: FREE PART OF THE *N*-*N* LOOP

Polarization tensors arising out of the n-$\bar{n}$ excitation of the Dirac sea:

$$\Pi^{vv}_{\mu\nu}=-\frac{1}{2}\left(\frac{g_v}{\pi}\right)^2\left[\frac{1}{3}(\Delta+\ln\mu^2)q^2Q_{\mu\nu}-2q^2Q_{\mu\nu}\int_0^1 dx x(1-x)\ln D\right], \tag{A1}$$

$$\Pi^{vt+tv}_{\mu\nu}=\frac{1}{2}\frac{g_v^2}{\pi^2}\frac{M^*\kappa_v}{2M}Q_{\mu\nu}\left[\Delta+\ln\mu^2-\int_0^1 dx\ln D\right], \tag{A2}$$

$$\Pi^{tt}_{\mu\nu}=-\frac{g_\rho^2}{(4\pi)^2}\left(\frac{\kappa}{M}\right)^2Q_{\mu\nu}\left[\frac{1}{6}q^2\left(\Delta+m^2\ln(\mu^2)-m^2+\frac{q^2}{q^2}+q^2\int_0^1 dx x^2\ln D-q^2\int_0^1 dx x\ln D-m^2\int_0^1 dx\ln D\right)\right], \tag{A3}$$

$$\Delta=\frac{1}{\epsilon}-\gamma+\ln 4\pi,$$

$$D=M^{*2}-q^2x(1-x).$$

All the terms containing Δ are infinite and need to be subtracted out.

APPENDIX B: FREE PART OF THE *N*-*R* LOOP

$$\Pi^{RN(\mathrm{dir})}_{\mu\nu}=Q_{\mu\nu}\Pi(q^2), \tag{B1}$$

where

$$\Pi(q^2,\mu)=(\Pi_1(q^2)+\Pi_2(q^2)+\Pi_3(q^2)+\Pi_4(q^2)+\Pi_5(q^2)+\Pi_6(q^2)+\Pi_7(q^2)+\Pi_8(q^2)), \tag{B2}$$

$$\Pi_1(q^2)=\left[(D+2x^2q^2)(\Delta+\ln m^2)+\int_0^1 dx(D-D\ln D-2q^2x^2\ln D)\right]\frac{q^2Q_{\mu\nu}}{32\pi^2} \tag{B3}$$

$$\Pi_2(q^2)=\left[2(3D^2+18Dq^2x^2+4q^4x^4)(\Delta+\ln\mu^2)+\int_0^1 dx(9D^2+36Dq^2x^2+6D^2\ln D-36Dq^2x^2\ln D-8q^4x^4\ln D)\right]\frac{q^2Q_{\mu\nu}}{128m_R^2\pi^2},$$

$$\Pi_3(q^2)=-\left[2q^2x(3D+2q^2x^2)(\Delta+\ln\mu^2)+\int_0^1 dx(3q^2xD-3q^2xD\ln D-2q^4x^3\ln D)\right]\frac{q^2Q_{\mu\nu}}{32m_R^2\pi^2},$$

$$\Pi_4(q^2)=-\left[(2D+q^2x^2)(\Delta+\ln\mu^2)+\int_0^1 dx(D-2D\ln D-q^2x^2\ln D)\right]\frac{q^2Q_{\mu\nu}}{16\pi^2},$$

$$\Pi_5(q^2)=-m_Nm_\Delta\left[(\Delta+\ln\mu^2)-\int_0^1 dx\ln D\right]\frac{q^2Q_{\mu\nu}}{16\pi^2},$$

$$\Pi_6(q^2)=\left[D(\Delta+\ln\mu^2)+\int_0^1 dx(D-D\ln D)\right]\frac{q^2Q_{\mu\nu}}{32\pi^2},$$

$$\Pi_7(q^2)=\left[2D(3D+2q^2x^2)(\Delta+\ln\mu^2)+\int_0^1\frac{dx}{m_R^2}D(9D+4q^2x^2-6D\ln D-4q^2x^2\ln D)\right]\frac{q^2Q_{\mu\nu}}{128\pi^2},$$

$$\Pi_8(q^2)=-\left[\int_0^1 dxDq^2x(\Delta+\ln\mu^2)+\int_0^1\frac{dx}{m_R^2}(Dq^2x-q^2xD\ln D)\right]\frac{q^2Q_{\mu\nu}}{32\pi^2}.$$

APPENDIX C: IDENTITIES INVOLVING RARITA-SCHWINGER SPINORS

$$\Delta^{\mu\nu}(p)=\sum\Psi^\mu(p)\bar{\Psi}^\nu(p)=(\not{p}+M_R)\left[-g^{\mu\nu}+\frac{1}{3}\gamma^\mu\gamma^\nu+\frac{2}{3}\frac{p^\mu p^\nu}{M_R^2}-\frac{1}{3}\frac{p^\mu\gamma^\nu-\gamma^\nu p^\mu}{M_R}\right]=(\not{p}+M_R)P^{\mu\nu}_{3/2}(p) \tag{C1}$$

$$\gamma_\mu P^{\mu\nu}_{3/2}(p)=\frac{1}{3M_R}(M_R^2-p^2)\left(\gamma_\nu-\frac{2p_\nu}{M_R}\right). \tag{C2}$$

Clearly the above and the following equations vanish when the spin 3/2 state is on-shell, so does Eq. (C3) also:

$$P^{\mu\nu}_{3/2}(p)\gamma_\nu=\frac{1}{3M_R}(M_R^2-p^2)\left(\gamma_\mu-\frac{2p_\mu}{M_R}\right). \tag{C3}$$

Another useful relation in this respect is the identity

$$(k-p)_\mu P^{\mu\nu}_{3/2}(p)(k-p)_\nu=\frac{2}{3}\frac{(p^2-M_R^2)}{M_R^2}[p^2-2k\cdot p] + \frac{2}{3M_R^2}[(k\cdot p)^2-M_R^2k^2]. \tag{C4}$$

It is to be noted that the above equation also takes a much simpler form when we have an on-shell spin 3/2 projection operator:

$$p_\mu\Psi^\mu(p)=0=\Psi^\nu(p)p_\nu, \tag{C5}$$

$$k_\mu P^{\mu\nu}_{3/2}(p)k_\nu=\frac{2}{3M_R^2}[(k\cdot p)^2-M_R^2k^2]. \tag{C6}$$

It is evident that $p_\mu P^{\mu\nu}_{3/2}(p)p_\nu=0$ when the spin 3/2 particle is on-shell, i.e., $p^2=M_R^2$. In the rest frame of the resonant state R, we, therefore, have $k_\mu P^{\mu\nu}_{3/2}k_\nu=\frac{2}{3}\mathbf{k}^2$.

[1] F. Klingl, N. Kaiser, and W. Weise, Nucl. Phys. **A624**, 527 (1997).
[2] A.K. Dutt-Mazumder, R. Hoffman, and M. Pospelov, Phys. Rev. C **63**, 015204 (2001).
[3] H. Shiomi and T. Hatsuda, Phys. Lett. B **334**, 281 (1994).
[4] R. Rapp and J. Wambach, Adv. Nucl. Phys. **25**, 1 (2000).
[5] M. Post, S. Leupold, and U. Mosel, Nucl. Phys. **A689**, 753 (2001).
[6] O. Teodorescu, A.K. Dutt-Mazumder, and C. Gale, Phys. Rev. C **61**, 051901(R) (2000).
[7] O. Teodorescu, A.K. Dutt-Mazumder, and C. Gale, Phys. Rev. C **63**, 034903 (2001).
[8] S.A. Chin, Ann. Phys. (N.Y.) **108**, 301 (1977).
[9] K. Saito, K. Tsushima, A.W. Thomas, and A.G. Williams, Phys. Lett. B **433**, 243 (1998).
[10] C. Gale and J.I. Kapusta, Nucl. Phys. **B357**, 65 (1991).
[11] See, for example, B.D. Serot, and J.D. Walecka, Adv. Nucl. Phys. **16**, 1 (1986).
[12] A. L. Fetter and J. D. Walecka, *Quantum Theory of Many-Particle Systems* (McGraw-Hill, New York, 1971).
[13] W. Peters, M. Post, H. Lenske, S. Leupold, and U. Mosel, Nucl. Phys. **A632**, 109 (1998).
[14] M.K. Banerjee and J. Milana, Phys. Rev. D **52**, 6451 (1995).
[15] P. Ellis and H. Tang, Phys. Rev. C **57**, 3356 (1998).
[16] T. Ericson and W. Weise, *Pions and Nuclei* (Oxford Science, Oxford, 1998).
[17] N. Isgur, C. Morningstar, and C. Reader, Phys. Rev. D **39**, 1357 (1989).
[18] R. Machleidt, Adv. Nucl. Phys. **19**, 198 (1989).
[19] M. Urban, M. Buballa, R. Rapp, and J. Wambach, Nucl. Phys. **A641**, 433 (1998).
[20] See, for example, R.J. Porter *et al.*, Nucl. Phys. **A638**, 499 (1998), and references therein.